

## Sterilization studies of hydrogel nanocomposites designed for possible biomedical applications before in vivo research

Gözde Bayazit Sekitmen<sup>a,\*</sup>, Esra Su<sup>b</sup>, Sinem Diken Gür<sup>c</sup>, Semra İde<sup>a,d</sup>, Oğuz Okay<sup>e</sup>

<sup>a</sup> Hacettepe University, Graduate School of Science and Engineering, Department of Nanotechnology and Nanomedicine, 06800 Beytepe, Ankara, Turkey

<sup>b</sup> Istanbul University, Faculty of Aquatic Sciences, Aquatic Biotechnology, 34134 Fatih, Istanbul, Turkey

<sup>c</sup> Hacettepe University, Faculty of Science, Department of Biology, 06800 Beytepe, Ankara, Turkey

<sup>d</sup> Hacettepe University, Faculty of Engineering, Department of Physics Engineering, 06800 Beytepe, Ankara, Turkey

<sup>e</sup> Istanbul Technical University, Faculty of Science, Department of Chemistry, 34469 Maslak, Istanbul, Turkey

### ARTICLE INFO

#### Keywords:

Nanostructures  
Hydrogels  
Physical sterilizations  
Formations of biofilm  
X-ray studies

### ABSTRACT

This study emphasized the importance of hydrogel-based therapy in repairing cartilage tissue and discussed the nanoscopic requirements for the physical sterilization of hydrogels, which are repairable, biochemically compatible with cartilage structure, and shape memory under mechanical effects.

The nanostructured and the shape memory hydrogel composites, previously designed, synthesized, and nano-structurally characterized by our group, were used as material in the present study. Samples are including poly (*N,N*-dimethylacrylamide) (poly (DMAA) chains, *n*-octadecyl acrylate (C18A) segments and with/without lauryl methacrylate (LM).

The study consists of four main sections in which physical sterilization processes (with electromagnetic waves from low energy (UV) to high energy (X-ray and Gamma-ray) are applied, structural changes are determined at microscopic and nanoscopic scale, and biofilm formations in the mentioned hydrogel materials are evaluated.

The present study investigated these hydrogels' potential as artificial cartilage or cartilage tissue scaffolds. To initiate in vivo studies, it was aimed to determine the most appropriate physical sterilization method.

In the result of the study, the most convenient hydrogel sample for surgical (in vivo) research, the useful physical sterilization methods, and the ability to resist biofilm formation was determined for the sample of N:3, [DMMA/C18A/LM, (70/30/0.0)] (Pre stretching ratio) = 1.8]. UV applications were also determined as the most generally suitable sterilization method for these hydrogels. As the pre-stretching ratio increases, the emergence of more compact and globular nano formations in hydrogel structures also affects the bioactive properties. It was also shown that, with the help of the usage of energetic electromagnetic waves for sterilizations, the new 3D nano aggregation morphologies might be created in the hydrogel structures.

### 1. Introduction

As known, mechanically strong hydrogels with anisotropic orientation and bioactive properties can be used as implants or scaffolds for many biological tissues such as skin, muscle, and cartilage [1]. Especially, their evaluation as cartilage in tissue engineering of the knee, big toe joints, lateral nasal cartilages, etc., have taken much interest in recent research [2]. On the other hand, instead of cartilage transplantation which creates new disorders in the biological tissue, hydrogel-based therapy may also be easier and better for correcting cartilage defects. The most important problem experienced after rhinoplasty operations is cartilage meltdown. Especially as an alternative

material for a modern rhinoplasty approach that does not use cartilage grafts, polymer-based, bioactive, mechanical properties optimized, and, most importantly, shape memory, new design nanomaterials can be recommended. [3,4]

Smart three-dimensional nanostructured hydrogel networks with programmable behavior can be used for the controlled delivery of therapeutics. Hydrogel swelling/shrinkage triggered by physicochemical (such as temperature and pH) effects is also effective in releasing some biochemical materials. Therefore, new hydrogel designs, dynamic structural behaviors, and functional properties are important in health-related developments (especially anti-cancer therapy). [5]

As mentioned in these studies, particularly shape memory hydrogel

\* Corresponding author.

E-mail address: [gozdebayazit@gmail.com](mailto:gozdebayazit@gmail.com) (G.B. Sekitmen).

<https://doi.org/10.1016/j.reactfunctpolym.2022.105393>

Received 13 June 2022; Received in revised form 23 August 2022; Accepted 6 September 2022

Available online 10 September 2022

1381-5148/© 2022 Elsevier B.V. All rights reserved.

materials that can form nanostructured networks have been focused on hydrogel materials because they are important in medical applications. [6–8]

Our previously designed and characterized (DMAA/C18A/LM) polymer-based hydrogel materials attain complex and nonlinear structures with anisotropic, viscoelastic properties and multiphase behaviors, which are expected for convenient alternative biomaterials for tissue engineering. These hydrogels have DMAA chains, connecting C18 segments to form crystalline domains and hydrophobic structures. So, such anisotropic hydrogels were used for their semicrystalline physical properties and shape memory function. [9,10]. Besides their extreme and useful properties, just before their usage in vivo studies, the sterilization research must be completed, and their biological activities must be determined.

This study was conducted as a preliminary study to reference in vivo experiments. Because the study aims to make scientific preparation by determining the most appropriate sterilization method required to initiate in-vivo studies, so, it is also necessary to determine the most suitable sterilization method before in vivo studies for such hydrogels whose original syntheses have been made, structure characterizations have been completed, and their 3D properties have been examined in detail. In the continuation of this study, in-vivo studies will be carried out.

In this study, a series of ( $N = 6$  pieces) hydrogel nanocomposites have been focused on, whose pioneering research has been completed [11,12]. For these novel composites to be used in in-vivo studies, it was determined in this study which of the physical sterilization methods met the expected biophysical functions without damaging the material's structure.

Any biomaterial needs to be suitable for efficient sterilization to obtain approval from the relevant organizations and to continue clinical trials safely [13]. The effects of sterilization on different types of hydrogels for biomedical applications also differ. It is necessary to perform tests according to the condition of the newly designed hydrogel materials to determine the most suitable and effective sterilization method that allows the main properties of the materials to remain unchanged [13].

It is known that sterilization processes based on liquid chemical sterilizers may not generally have the same level of sterility assurance. Therefore, physical methods are widely preferred [14].

Fig. 1 shows the main physical sterilization methods, including the used methods in the present study.

UV, X-Ray, and Gamma Rays were used in physical sterilization methods. The use of these three different electromagnetic waves brings different advantages and disadvantages. While the energetic rays penetrate deeply into the structure, they cause damage to the material at the atomic and molecular levels. In addition, it is previewed that during the irradiation process, the emergence of new nano-formations in the

structure and the new structure arrangements formed during the irradiation process may positively change the material's properties. Studies on the emergence of specific stable nano arrangements, increasing crystallinity, and triggering the formation of new nanoclusters, especially in nanoscopic structures exposed to long-term radiation, have been reported in the literature [15,16].

Although X-Ray is a 100-year-old technology, its use in the industry for sterilization of medical materials is very new. In this context, the evaluation of the effectiveness of the use of X-rays in both sterilization and nanoscopic analysis is the unique approach in this study.

3D nanoscopic aggregations in the hydrogel samples may be effectively and deeply followed by SAXS analyses [17,18]. Compared to a material's atomic and molecular structures, it is known today that the nanostructure is the most effective in the superior properties of that material [19]. Hydrogels can act as macromolecular structures by responding rapidly to external stimuli, making them worthy of study as more functional or smarter materials. So, the nanoscopic structural changes under the effect of the physical sterilizations were investigated by SAXS analyses.

The development of biofilm-associated infections for patients with implemented artificial materials causes an urgency to develop coatings or treatments with high antibiofilm activity for improving the used materials [20]. In this study, to determine the biofilm preventing efficiency of the treated hydrogel materials designed by our research group, *Staphylococcus aureus* (*S. aureus*) ATCC 25923, one of the most common pathogens [21] involved in bone and joint infections, was used. A modified crystal violet assay was performed to quantify the biofilm mass of *S. aureus* biofilm formed on the treated cartilages.

## 2. Materials and methods

### 2.1. Hydrogel samples

Two hydrogel groups with different molar ratios of the hydrophilic *N*, *N*-dimethylacrylamide (DMAA) monomer, strong and weak hydrophobic *n*-octadecyl acrylate (C18A), and lauryl methacrylate (LM) monomers, respectively, were previously synthesized as a part of our research projects [5,6]. The precursor hydrogels consist of poly (DMAA) chains interconnected by C18A segments forming crystalline domains and acting as switching segments with/without LM units as the net-points. Shortly, the hydrogels were synthesized by bulk photopolymerization of DMA, C18A, and LM in the presence of Irgacure 2959 as a photoinitiator at a wavelength of 360 nm. After a polymerization time of 24 h, all the monomers completely converted to a water-insoluble terpolymer. After equilibrium swelling in water, semi-crystalline isotropic hydrogels (prestretch ratio  $\lambda = 1$ ) with water contents between 26 and 37 wt% were obtained. To obtain prestretched anisotropic hydrogels, the isotropic hydrogel specimens were stretched in water at 80 °C to a predetermined strain and then immersed in a water bath at 20 °C by fixing the strain. The details about the studied hydrogel samples are given in Table 1.

All samples include nanoscaled crystallite formations, and the size, shape, and distributions change according to the stretching and the sample groups. The samples are stable and exhibit shape memory under the mechanical effects.

**Table 1**

The studied hydrogel samples. The molar ratios of the monomers are given in parenthesis.

Two sample groups (DMAA/C18A/LM)	Prestretch ratio ( $\lambda$ )	Sample code, N
70/30/0.0	1.8	3
	1.2	4
	0.0	5
70/29.9/0.1	0.0	6
	1.2	7
	1.8	8

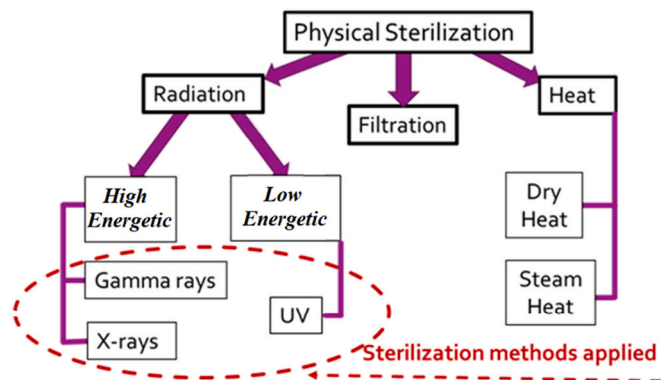


**Fig. 1.** Widely used physical sterilization methods and the applied methods for the focused hydrogels.

The molecular and nanostructural models of the samples are also summarized in Fig. 2.

These hydrogels were also focused on due to their biochemical similarities to cartilage tissue besides the above-mentioned physical properties.

## 2.2. Sterilizations

In UV sterilization processes, experimental conditions with 200–400 nm wavelengths and irradiation energy transfer in the range of 2.59–6.48 J/cm<sup>2</sup> were created. This method indicates several advantages because of its widely used, high antimicrobial effect, the cheapest experimental applications, and low destruction in the samples.

In X-Ray sterilization processes, the HECUS system source-off X-Ray tube was used again with 8 keV energy. The exposure time was 20 min. for photon flux of 106 photon/mm<sup>2</sup>/s. It is a new alternative sterilization method for industrial products and systems, with its high penetration into the material, the ability to prevent damage with controlled flux and violence to prevent damage, the possibility of making dynamic and rapid measurements, the ability to form new hydrogen bonds with irradiation and cause more stable structures which can be considered as the advantage of the method.

In gamma irradiation, a Co-60 source (12 kGy) was used in the Gamma Irradiation facility at Nuclear Energy Research Institute in Turkey. The most important advantages of sterilization processes using gamma rays can be mentioned as “Highest penetration (controlled energy and path length), Direct application, Zero persistent radioactivity after application, Experimentally simple implementation (no controls required for T, P, humidity, vacuum, etc.)”.

## 2.3. Microscopic research

Scanning electron microscope (SEM) images (Fig. 3) have contributed to the three-dimensional illumination of the superstructure of hydrogel materials. As can be seen from the figure, the surface morphologies of the material (N:8) are mostly affected by different physical sterilization applications. So, this sample was chosen to compare the control group and sterilized samples with different methods.

The SEM images (with a 2 μm scale) were obtained by GAIA3-TESCAN at HUNITEK center with experimental conditions of 5.0 kV,

10.4-μm view field, MAG: 20.0 k x, Scan speed 6, and Det: SE.

## 2.4. SAXS analyses

The intensities of the scattered X-rays,  $I(q)$ , were recorded on a HECUS-SAXS (Kratky optic) Camera’s line collimation detector with 1024 channels. The solid phase hydrogel samples with each size of 5x3x1 mm were in convenient sample holders. Different orientations of the samples were also tested, and all samples were measured to obtain the best 3D nano globular morphologies because of the complicated 3D aggregations in the hydrogels. The scattering curves were plotted as  $I(q)$  vs.  $q$ ; where  $q = 4\pi\sin\Theta/\lambda$  and  $2\Theta$ : the angle between the incident and scattered beam. X-ray with a wavelength of (CuK $\alpha$ ) 1.54 Å was used in scattering measurements. The SAXS profiles of the N:3 sample before and after X-ray sterilization were plotted, as seen in Fig. 4, to show the effect of the sterilization on a nanoscopic scale. All scattering data may be obtainable from the corresponding author.

The 3D ab-initio electron density morphologies were obtained using the Indirect Fourier Method [22] and DAMMIN software. [23]

In such studies, structural analysis at the molecular level is generally performed with spectroscopic methods, and the XRD method is also used for crystallinity analyses. To examine nano and micro-scale structural changes, only very small parts of the material to be used (called a needle tip) can be compared with microscopic techniques or surface analysis. However, since the sample size examined by SAXS analysis is 8x5x1 mm, the structural change findings cover a full size that can be considered a macroscopic structure. In addition, with the SAXS method, nanoscopic formations with structural changes in the electron density level can be examined in 3 dimensions, and important structural findings such as morphology, size, and distance distribution can be reached. A similar study has been done for dental grafts in one of our recent publications. [24]

## 2.5. Biofilm formations

Since biofilm formation in living organisms is associated with tissue and implant infections, it is also important to examine biofilm formations in studied hydrogels, which are likely to be used as implants or tissue scaffolds before in-vivo studies.

The first step required for biofilm formation is the adhesion of the

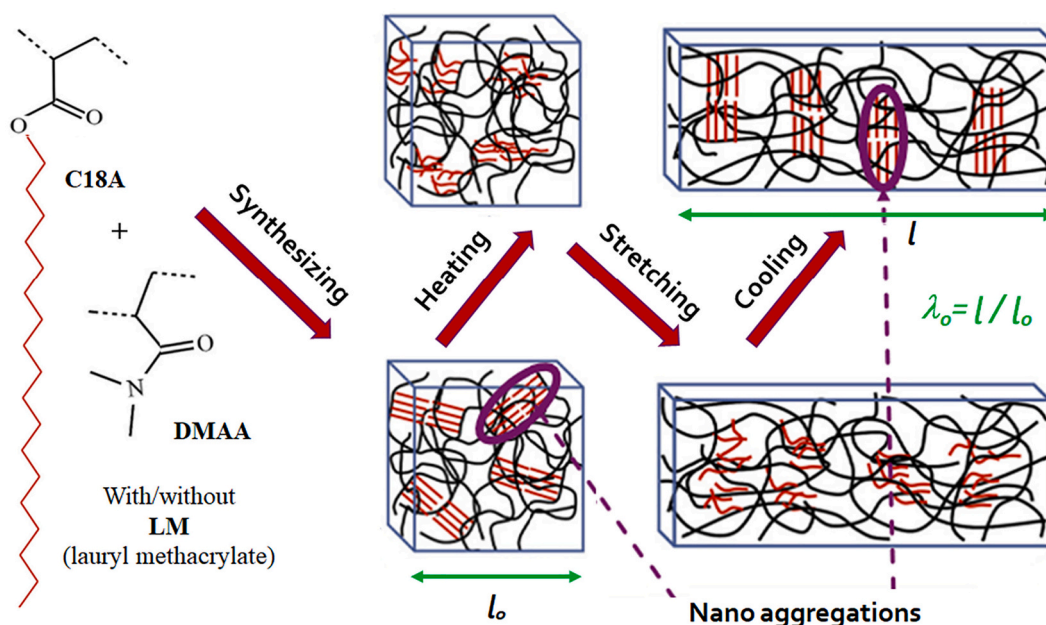


Fig. 2. The molecular and nanoscopic structure of the samples.



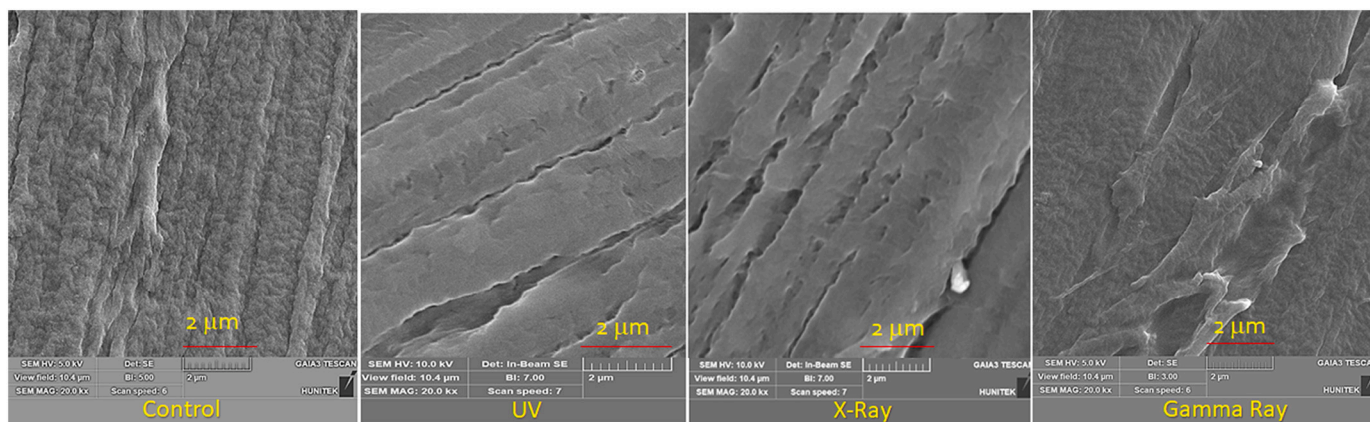


Fig. 3. SEM images (N:8) related to the different sterilizations' effects on the surface morphologies of the hydrogels.

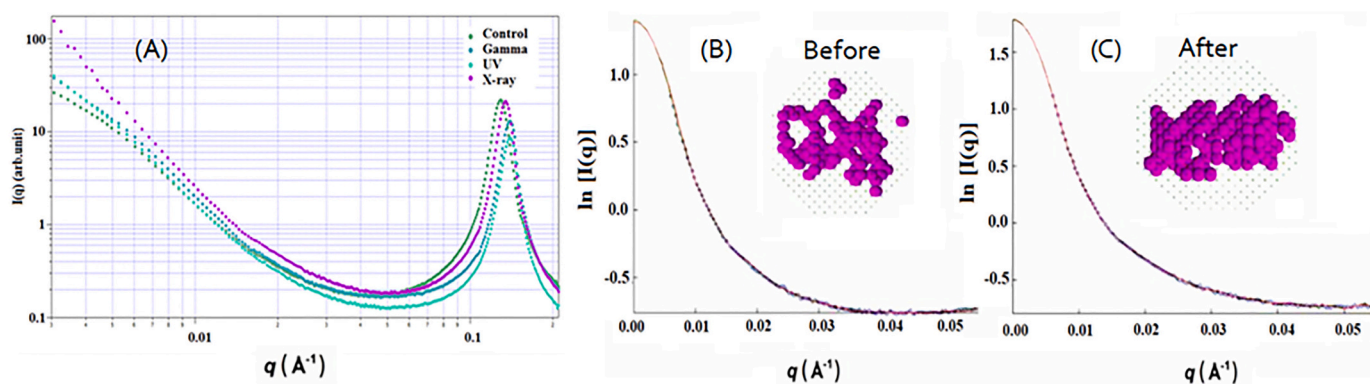


Fig. 4. A) SAXS profiles, B) and C) fitting curves, and the obtained 3B nano globular morphologies before and after X-ray sterilization for the N:3 sample [(70/30/0.0) and prestretching ratio: 1.8].

microorganism to the surface. Such biofilm formation in implant or graft materials is a major source of tissue infections. [25] Common components required for forming a biofilm are microorganisms, glycocalyx, and surface. Biofilm does not form when any of these components is absent. [26,27]

In biofilm formation, bacteria do not fully contact the surface, and long-distance interactions occur between the bacteria and the surface. These are hydrophobic, and Van der Waals bonds and are weak interactions. Hydrophobic interactions have an important place in the first

contact with the surface. Such interactions occur when there is a 10–20 nm distance between the surface and the bacteria. In addition, the surface must be rough or smooth for initial bacterial adhesion because the rough surface in the first adhesion increases the probability of adhesion. In other words, the surface roughness of the implants affects the young biofilm adhesion and triggers biofilm formation (bioplaque). [28]

Fig. 5 shows the images of *Staphylococcus aureus* (*S. aureus*) ATCC 25923 applications on the focused hydrogel materials. A modified crystal violet assay was performed to quantify the biofilm mass of

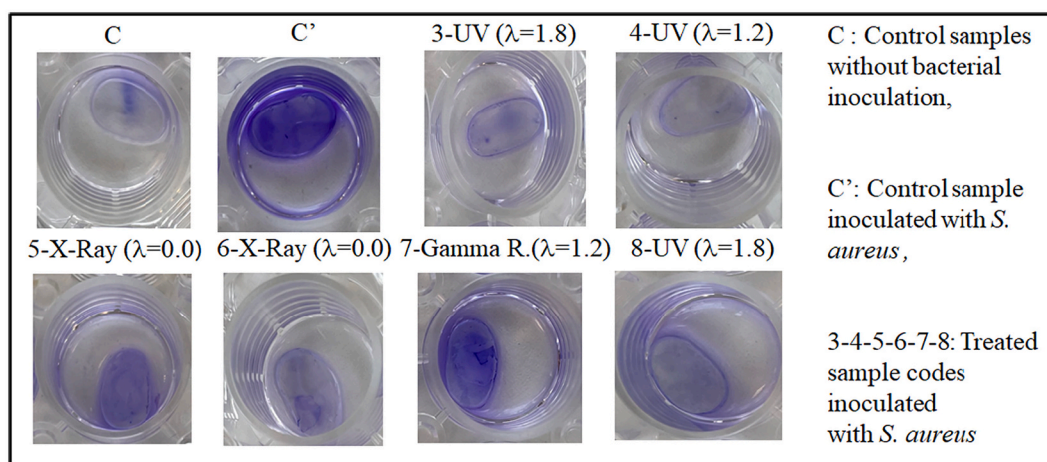


Fig. 5. Observations related to the bacterial adhesion in the darkly stained areas.

*S. aureus* biofilm formed on the treated samples. The bacterial adhesion in the darkly stained areas may also be seen in Fig. 5. Biofilm quantities formed by *S. aureus* after 24 h incubation on the five hydrogel samples with different surface structures.

### 3. Result and discussion

Electromagnetic waves (EMW) like x-ray, gamma and UV pass through the material to transfer its energy through ohmic loss. This energy causes conduction electron current formation in the material. Hydrogel structures are not suitable for forming regular currents because their lattice vibrations of microcrystalline regions can also be excited by the electric field oscillation of the applied EMW, and EMW energy can be absorbed by developing a thermal effect. In this case, movements in the structure in the crystalline regions and changes in the morphology of nanoscopic formations may occur.

In sterilization processes, gamma and X-rays affect the nuclei and inner electrons (respectively) of the atoms in the hydrogel and bacteria structures. However, UV light can play a more active role in the interaction of the implant surface and the bacterial envelope at nanoscopic distances by directly affecting the outer electrons in atomic structures. For example, the formation of van der Waals bonds will become a more difficult result of the excitation caused by the UV effect between the implant or graft surface that comes close to contact (10–20 nm) and the bacteria. UV effect and stimulation do not show very stable and long-term results in affecting bacterial adhesion and biofilm formation, as it has lower energy. Gamma rays are also high-energy, and since they directly affect the nuclei of atoms in the material, they can also cause damage to the implant structure, so the use of these rays should always be controlled. However, by using X-Ray, the short-term effects of UV rays on biofilm formation can be further improved, and the damage caused by gamma rays can be minimized.

The following structural results and interpretations were given according to the different scales of the electromagnetic wave response in the sterilization process.

#### 3.1. Microscopic and nanoscopic evaluations

It has been determined that the applied physical sterilization methods can cause visible and invisible changes on microscopic and nanoscopic scales (Figs. 3, 4). The microscopic effect in which this structural change was most observed occurred in the N:8 sample.

Our previously published SAXS analyses on newly designed hydrogel samples are evidence of the importance of nano-scaled structural analyses by the SAXS method [29,30]. The most apparent sterilization effect in the nanoscopic structure was observed in the globular compact form in the N:3 sample. Fig. 6 provides visual information on this subject.

The most general results and comparisons may be followed in Fig. 7 for nanoscopic analyses. The similarities in the 3B models (related to nanocrystalline aggregations) indicate successful nanostructures, which are evidence of undestroyable effects and unwanted structural deviations in real functional structures [31].

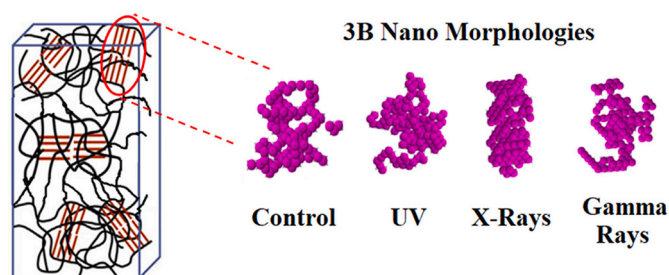


Fig. 6. Comparison of the effects of different sterilization processes (N:3 composite) on nanostructure.

So, it was determined that in the nanoscale structure; the closest structural change to the control group occurred with UV sterilization (with three green stars), and deterioration in the structure occurred due to the effect of gamma rays and in X-ray applications (as expected because of their higher energies), crystallite morphologies formed as more compact structures that would increase the mechanical properties of the material.

In one of our previous studies, gamma-ray sterilization was very successful on dental graft materials [26]. However, in this study, only N:4 and N:7 samples showed nanostructures close to control samples, and this means that the gamma-ray effects on biomaterials can vary with the materials and their different mechanical properties.

On the other hand, with the sterilization effect of energetic X-rays and gamma rays in N: 4 and 8 samples, the structure of the control sample reaches more compact nano formation morphologies (Fig. 7). In other words, these rays trigger the nano-formations to be more voluminous (globular) and the concentration of electron-dense aggregations to central points. This situation enables the establishment of new bonds by transferring energy to electrons at high frequencies, freeing them from their weakly bonded structure and triggering new atomic and molecular interactions that will cause a more global minimum energy [15,16].

In addition, SEM photographs of the sample code 8, control group, and sterilized samples with different methods support the SAXS analysis. It can be seen in Fig. 3 the difference between the control group and other samples. On a 2  $\mu\text{m}$  scale, all sterilization methods changed the surface morphology (it is seen that the lines are widened), but the most degradation is seen in x-ray sterilization methods. A significant change in macro dimensions was not observed in other samples. Therefore, SAXS analyses were also performed to examine the changes on the nanoscale.

#### 3.2. Evaluations on biofilm formations

The structural determinations were collaboratively combined with the biofilm investigation on the hydrogel surfaces. Fig. 8 shows the quantitative results related to this examination. After the sterilization of the hydrogels, for their usage in biomedical applications, bacterial adhesion on the surfaces must be prevented.

The treatment applied to sample 6-X-Ray ( $\lambda = 0.0$ ), 4-UV ( $\lambda = 1.2$ ), and 3-UV ( $\lambda = 1.8$ ) that were prepared without any antibacterial agent have enhanced their ability to reduce adhesion of bacteria and gained strong antibiofilm activity to these hydrogels against *Staphylococcus aureus*. The development of hydrogels using hydrophilic polymer (DMAA) promote not only the structural stability of prepared hydrogel but also eliminate the risk of resistant bacteria growth associated with the use of antibacterial agent by acting as an antifouling material against bacterial adhesion. [32]

According to the results shown in Fig. 8, the least biofilm formation was observed for N:6. However, the nanoscale structures deviate from the real functional nanostructure of the control group after X-Ray treatment, as seen in Fig. 7 (for N:6). Therefore, the loss of structural stability of the N:6 sample limits its use as artificial cartilage or tissue scaffold.

When the 3D nanostructural changes and antibiofilm properties were analyzed, hydrogel sample N:3 was determined to be the most suitable candidate for biomedical applications. Although the least nanoscopic structure differences from the control sample were recorded for N:3, it was observed that p(DMAA) showed enhanced antiadhesion properties after UV sterilization. In recent studies, it was emphasized that UV sterilization increases the hydrophilicity of the different materials. [33,34] It is a known fact that all bacteria tend to adhere more strongly to hydrophobic surfaces, even if they have different cell wall structures [35] So, hydrogel developed in this study with enhanced hydrophilicity could prevent bacterial adhesion with a perfect antibiofilm capability.

In line with obtained results, it has been decided to use the N:3

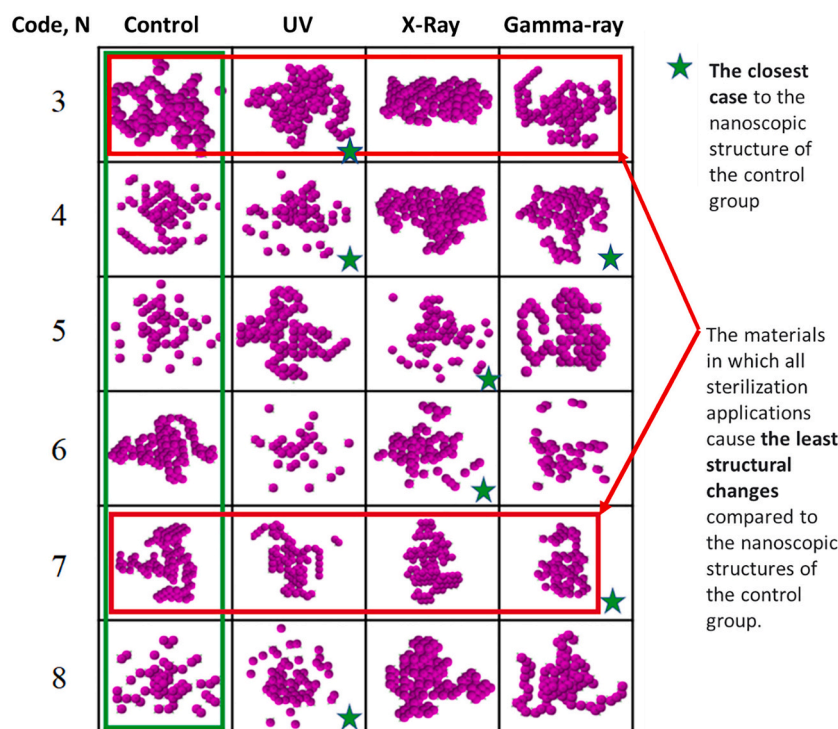


Fig. 7. Comparison of the effects of different sterilization methods on nanostructures according to the nanoglobular findings determined in the control group.

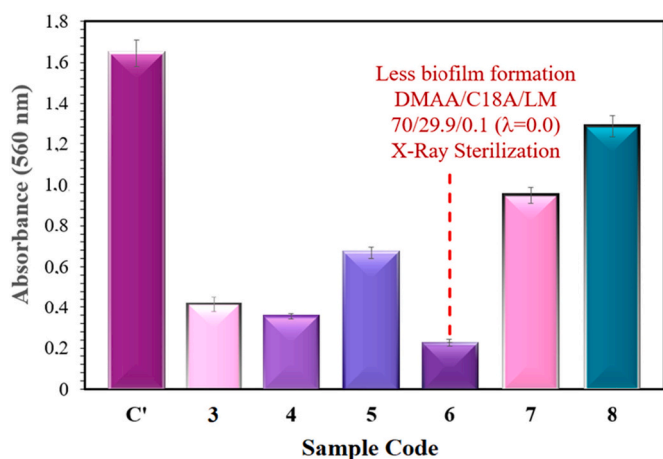


Fig. 8. Quantitative results according to the treated samples.

sample for biomedical approaches in a future planned research. For example, new studies on the adhesion of some protein structures to this hydrogel material before surgical applications can be initiated by our group.

#### 4. Conclusion

In biomedical applications, any technological material that will enter the human body must be made of structural analyses at a nanoscopic scale, structure-function relationships must be taken under control, and materials suitable for sterilization studies. When such materials are used as tissue scaffolds or direct implants, they must first be stable against mechanical effects and should not undergo structural changes for a long time with their shape memory properties since they will be in a dynamic environment.

This study tried to determine the most effective physical sterilization

method for in-vivo studies to investigate the potential uses of our previously designed hydrogel materials as cartilage tissue implants or tissue scaffolds.

Consequently, it was determined that different sterilization methods could be effective in hydrogels prepared with different mechanical effects. In other words, on some materials, UV was effective, while X-Rays or gamma rays sterilizations were more successful in others.

As another result, it was declared that the presence of volumetric crystallite formations in nanoscopic sizes, which are formed due to physical sterilization applications using incredibly high-energy radiation in the studied hydrogel structures, may open new ways to design novel nanostructured hydrogels. For example, hydrogel structures containing ellipsoidal nanostructures can easily prepare with these materials and appropriate energetic electromagnetic wave applications such as X-rays and gamma rays.

It was also determined that biofilm formation in the materials could be controlled according to the external mechanical effects applied during the preparation of the designed hydrogels. It was also declared that these bio-functional controls could be made by changing the pre-stretching value.

With this study, our project-based original designed hydrogel material with shape memory was made ready for in-vivo studies at the initial stage. In the next phase, studies on protein-hydrogel interactions and bioactivity will be able to emphasize, too. In future studies, the synthesis of novel hydrogels, including removable nanocrystallites, may be realized by our group to design pH or thermoresponsive drug delivery systems and materials.

#### Authors statement

The manuscript REACT-D-22-00473 (Sterilization Studies of Hydrogel Nanocomposites Designed for Possible Biomedical Applications Before In Vivo Research) was written through contributions of all authors. All authors have given approval to the final version of the manuscript.



## CRediT authorship contribution statement

**Gözde Bayazit Sekitmen:** Investigation, Data curation, Writing – review & editing. **Esra Su:** Methodology, Data curation. **Sinem Diken Gür:** Data curation, Methodology, Writing – review & editing. **Semra İde:** Conceptualization, Methodology, Writing – original draft, Writing – review & editing, Supervision. **Oğuz Okay:** Visualization, Methodology, Writing – review & editing.

## Declaration of Competing Interest

The authors declare that they have no known competing financial interests or personal relationships that could have appeared to influence the work reported in this paper.

We have no conflicts of interest to disclose.

## Data availability

Data will be made available on request.

## Acknowledgements

The work was supported by the Scientific and Technical Research Council of Turkey (TUBITAK), KBAG 114Z312, Istanbul Technical University, BAP TDK-2017-40506, and by Hacettepe University, BABK project (FHD-2020-18669) and it includes a part of G.B. Sekitmen's doctoral work which is also related to gaining experience in nanoscopic analysis.

## References

- [1] K. Sano, Y. Ishida, T. Aida, Synthesis of anisotropic hydrogels and their applications, *Angew. Chem. Int. Ed.* 57 (10) (2018) 2532–2543, <https://doi.org/10.1002/anie.201708196>.
- [2] S.A. Hosseini, R. Mohammadi, S. Noruzi, R. Ganjif, F. Oroojaliang, A. Sahebkar, Evolution of hydrogels for cartilage tissue engineering of the knee: a systematic review and meta-analysis of clinical studies, *Joint Bone Spine* 88 (2021), 105096, <https://doi.org/10.1016/j.jbspin.2020.105096>.
- [3] M.A. Altay, S. Sipahioğlu, C. Ertürk, N. Altay, K. Yüce, A. Levent, B.V. Çetin, Short term outcomes of arthroscopic repair of cartilage injury in knee using resorbable polymer implants, *Turkiye Klinikleri J. Orthop. Traumatol. Special Topics* 9 (1) (2016) 49–55.
- [4] C.E. Quatman, J.D. Harris, T.E. Hewett, Biomechanical outcomes of cartilage repair of the knee, *J. Knee Surg.* 25 (3) (2012) 197–206, <https://doi.org/10.1055/s-0032-1322602>.
- [5] M. Arjama, S. Mehnath, M. Jeyaraj, Self-assembled hydrogel nanocube for stimuli responsive drug delivery and tumor ablation by phototherapy against breast cancer, *Int. J. Biol. Macromol.* 213 (435–446) (2022), <https://doi.org/10.1016/j.ijbiomac.2022.05.190>, 0141–8130.
- [6] S. Mehnath, M. Arjama, M. Rajan, M. Jeyaraj, Development of cholate conjugated hybrid polymeric micelles for FXR receptor mediated effective site-specific delivery of paclitaxel, *New J. Chem.* 42 (2018) 17021–17032, <https://doi.org/10.1039/C8NJ03251C>.
- [7] S. Mehnath, M. Rajan, G. Sathishkumar, R.A. Praphakar, M. Jeyaraj, Thermoresponsive and pH triggered drug release of cholate functionalized poly (organophosphazene) - polylactic acid copolymeric nanostructure integrated with ICG, *Polymer* 133 (2017) 119–128, <https://doi.org/10.1016/j.polymer.2017.11.020>.
- [8] A. Mukherjee, S. Mehnath, R. Mariappan, M. Jeyaraj, Injectable cuttlefish HAP and macromolecular fibroin protein hydrogel for natural bone mimicking matrix for enhancement of osteoinduction progression, *React. Funct. Polym.* 160 (2021), 104841, <https://doi.org/10.1016/j.reactfunctpolym.2021.104841>.
- [9] E. Su, C. Bilici, G. Bayazit, S. İde, O. Okay, Solvent-free UV polymerization of n-octadecyl acrylate in butyl rubber: a simple way to produce tough and smart polymeric materials at ambient temperature, *ACS Appl. Mater. Interfaces* 13 (18) (2021) 21786–21799, <https://doi.org/10.1021/acsmi.1c03814>.
- [10] E. Su, G. Bayazit, S. İde, O. Okay, Butyl rubber-based interpenetrating polymer networks with side chain crystallinity: self-healing and shape-memory polymers with tunable thermal and mechanical properties, *Eur. Polym. J.* 168 (4) (2022), 111098, <https://doi.org/10.1016/j.eurpolymj.2022.111098>.
- [11] C. Bilici, D. Karaarslan, S. İde, O. Okay, Toughness improvement and anisotropy in semicrystalline physical hydrogels, *Polymer* 151 (2018) 208–217, <https://doi.org/10.1016/j.polymer.2018.07.077>.
- [12] C. Bilici, S. İde, O. Okay, Yielding behavior of tough semicrystalline hydrogels, *Macromolecules* 50 (2017) 3647–3654, <https://doi.org/10.1021/acs.macromol.7b00507>.
- [13] R. Galante, T.J.A. Pinto, R. Colaço, A.P. Serro, Sterilization of hydrogels for biomedical applications: a review, *J. Biomed. Mater. Res. B Appl. Biomater.* 106 (6) (2018) 2472–2492, <https://doi.org/10.1002/jbm.b.34048>.
- [14] W.A. Rutala, D.J. Weber, the Healthcare Infection Control Practices Advisory Committee (HICPAC), *Guideline for Disinfection and Sterilization in Healthcare Facilities*, 2019, p. 163.
- [15] H. Cuie, H.T. Pashuck, Y.S. Velichko, S.J. Weigand, A.G. Cheetham, C.J. Newcomb, Spontaneous and X-ray-triggered crystallization at long range in self-assembling filament networks, *Science* 327 (2010) 555–559, <https://doi.org/10.1126/science.1182340>.
- [16] S.-Ja Tseng, Chia-Chi Chien, Zi-Xian Liao, Hsiang-Hsin Chen, Yi-Da Kang, Cheng-Liang Wang, Y. Hwu, G. Margaritondo, Controlled hydrogel photopolymerization inside live systems by X-ray irradiation, *Soft Matter* 8 (2012) 1420–1427, <https://doi.org/10.1039/c1sm06682j>.
- [17] C. Huerta-López, J. Alegre-Cebollada, Protein hydrogels: the Swiss army knife for enhanced mechanical and bioactive properties of biomaterials, *Nanomaterials* 11 (2021) 1656, <https://doi.org/10.3390/nano11071656>.
- [18] M. Roessle, D.I. Svergun, Small angle X-ray scattering, in: G.C.K. Roberts (Ed.), *Encyclopedia of Biophysics*, Springer Science and Business Media LLC, 2013, pp. 2382–2389.
- [19] C.S.A. De Lima, T.S. Balogh, J.P.R.O. Varca, G.H.C. Varca, A.B. Lugaõ, L. Camacho, L.A. Cruz, E. Bucio, S.S. Kadlubowski, An updated review of macro, micro, and nanostructured hydrogels for biomedical and pharmaceutical applications, *Pharmaceutics* 12 (10) (2020) 970, <https://doi.org/10.3390/pharmaceutics12100970>, 28.
- [20] S. Targonska, J. Rewak-Soroczynska, A. Piecuch, E. Paluch, D. Szymanski, R. J. Wiglus, Preparation of a new biocomposite designed for cartilage grafting with antibiofilm activity, *ACS Omega* 5 (2020) 24546–24557, <https://doi.org/10.1021/acsomega.0c03044>.
- [21] B.A. Pati, W.E. Kurata, T.S. Horseman, L.M. Pierce, Antibiofilm activity of chitosan/epsilon-poly-L-lysine hydrogels in a porcine ex vivo skin wound polymicrobial biofilm model, *Wound Rep. Reg.* 29 (2021) 316–326, <https://doi.org/10.1111/wrr.12890316>.
- [22] S.P. Meisburger, X. Da, N. Ando, Regals: a general method to deconvolve X-ray scattering data from evolving mixtures, *IUCr. J.* 8 (2021) 25–237, <https://doi.org/10.1107/S2052252521000555>.
- [23] D.I. Svergun, Restoring low resolution structure of biological macromolecules from solution scattering using simulated annealing, *Biophys. J.* (1999) 2879–2886, [https://doi.org/10.1016/S0006-3495\(99\)77443-6](https://doi.org/10.1016/S0006-3495(99)77443-6).
- [24] S. Bargh, M. Silindir-Gunay, A.Y. Ozer, E. Palaska, D. Karaarslan, S. İde, D. Solpan, Physicochemical evaluation of gamma and microwave irradiated dental grafts, *Radiat. Phys. Chem.* 170 (2020), 108627, <https://doi.org/10.1016/j.radphyschem.2019.108627>.
- [25] M.O. Kartal, B. Ekinci, B. Poyraz, Biofilm structure and prevention, *Akad. Gıda* 19 (3) (2021) 353–363, <https://doi.org/10.24323/akademik-gida.1011231>.
- [26] Dunne WM Jr., Bacterial adhesion: seen any good biofilms lately? *Clin. Microbiol. Rev.* 15 (2) (2002) 155–166, <https://doi.org/10.1128/CMR.15.2.155-166.2002>.
- [27] R. Funari, A.Q. Shen, Detection and characterization of bacterial biofilms and biofilm-based sensors, *ACS Sensors* 7 (2) (2022) 347–357, <https://doi.org/10.1021/acssensors.1c02722>.
- [28] E.Y. Dosdoğru, A.P. Erdem, E. Sepet, Z. Aytepe, Effects of different restorative materials on dental biofilm, *Atatürk Üniversitesi Diş Hekimliği Fakültesi Dergisi* 24 (8) (2015) 89–97, <https://doi.org/10.17567/dfd.39339>.
- [29] M. Goktas, G. Cinar, I. Orujalipoor, S. İde, A.B. Tekinay, M.O. Guler, Self-assembled peptide amphiphile nanofibers and PEG composite hydrogels as tunable ECM mimetic microenvironment, *Biomacromolecules* 16 (4) (2015) 1247–1258, <https://doi.org/10.1021/acs.biomac.5b00041>.
- [30] S. Ustun Yaylaci, M. Sardan Ekiz, E. Arslan, N. Can, E. Kilic, H. Ozkan, I. Orujalipoor, S. İde, A.B. Tekinay, M.O. Guler, Supramolecular GAG-like self-assembled glycopeptide nanofibers induce chondrogenesis and cartilage regeneration, *Biomacromolecules* 17 (2) (2016) 679–689, <https://doi.org/10.1021/acs.biomac.5b01669>.
- [31] S. Bargh, M. Silindir-Gunay, A.Y. Ozer, E. Palaska, D. Karaarslan, S. İde, D. Solpan, Physicochemical evaluation of gamma and microwave irradiated dental grafts, *Radiat. Phys. Chem.* 170 (2020), 108627, <https://doi.org/10.1016/j.radphyschem.2019.108627>.
- [32] K. Yu, A. Alzahrani, S. Khoddami, D. Ferreira, K.B. Scotland, J.T. Cheng, H. Yazdani-Ahmadabadi, Y. Mei, A. Gill, L.E. Takeuchi, E. Yeung, Self-limiting mussel inspired thin antifouling coating with broad-spectrum resistance to biofilm formation to prevent catheter-associated infection in mouse and porcine models, *Adv. Healthcare Mater.* 10 (6) (2021) 2001573, <https://doi.org/10.1002/adhm.202001573>.
- [33] A. Han, J.K. Tsoi, J.P. Matinlinna, Y. Zhangand, Z. Chen, Effects of different sterilization methods on surface characteristics and biofilm formation on zirconia in vitro, *Dent. Mater.* 34 (2) (2018) 272–281, <https://doi.org/10.1016/j.dental.2017.11.012>.
- [34] C. Krömmelbein, M. Mütze, R. Konieczny, N. Schönherr, J. Griebel, W. Gerdes, S. G. Mayr, S. Riedel, Impact of high-energy electron irradiation on mechanical, structural and chemical properties of agarose hydrogels, *Carbohydr. Polym.* 263 (2021), 117970, <https://doi.org/10.1016/j.carbpol.2021.117970>.
- [35] R. Gharibi, S. Agarwal, Favorable antibacterial, antibiofilm, antiadhesion to cells, and biocompatible polyurethane by facile surface functionalization, *ACS Appl. Bio Mater.* 4 (5) (2021) 4629–4640, <https://doi.org/10.1021/acsbm.1c00356>.